J Mater Sci (2009) 44:6546–6552
DOI 10.1007/s10853-009-3681-7

MESOSTRUCTURED MATERIALS

Synthesis of mesoporous aluminophosphates impregnated with metals and their application in gas oil desulphurization by adsorption

V. I. Águeda · J. L. Sotelo · M. A. Uguina · R. Rodríguez

Received: 28 November 2008 / Accepted: 12 June 2009 / Published online: 30 June 2009

Abstract Mesoporous materials based on aluminophosphates and silicates have been synthesised and impregnated with different loadings of transition metals such as Ag, Cu and Ni. These materials have been characterised and tested as selective adsorbents for the desulphurization of light cycle oil (LCO) by liquid adsorption. The polarity of the adsorbent matrix showed a positive effect on desulphurization, leading the impregnated aluminophosphates to higher adsorption capacities than the silicates. Among the transition metals tested, Ag-impregnated materials showed the best results followed by Cu and Ni. The aluminophosphate synthesised using pluronic F-127 block copolymer impregnated with a 5% of Ag (MFAP-5Ag) presented the best adsorption results with a maximum adsorption capacity of 11.36 mg S/g of adsorbent (equilibrium experiments), and breakthrough and saturation capacities of 4.25 mgS/g and 7.06 mgS/g, respectively (dynamic experiments).

List of symbols

C	Sulphur concentration, ppmw
FBU	Fractional bed utilisation; defined as q_{br}/q_{sat}
K	Equilibrium constant, ppm^{-n}; parameter defined in Eq. 1
n	Langmuir-Freundlich exponent; parameter defined in Eq. 1
q_D	Adsorption capacity, mg g^{-1}
$q_{D.eq}$	Adsorption capacity from the isotherm at a given concentration, mg g^{-1}
q_{max}	Maximum adsorption capacity, mg g^{-1}; parameter defined in Eq. 1
DES	Degree of desulphurization, %
t	Time, min

Subscripts and superscripts

0	Initial
br	Breakthrough time
eq	Equilibrium
sat	Saturation time

V. I. Águeda (✉) · J. L. Sotelo · M. A. Uguina · R. Rodríguez
Chemical Engineering Department, Faculty of Chemistry, Complutense University of Madrid, 28040 Madrid, Spain
e-mail: viam@quim.ucm.es

Introduction

European legislation limits sulphur content in road fuels to 50 ppmw. This will be reduced to 10 ppmw by 2009 (European Directive 2003/17/CE). However, sulphur concentrations below 1 ppmw have to be achieved for the application of fuels in fuel cell technologies because sulphur would poison the catalysts involved in the process [1]. Hydrodesulphurization (HDS) process is extensively used to remove sulphur in fuels. Nevertheless, some sulphur compounds as alkyldibenzothiophenes cannot be removed easily, so alternative technologies must be developed [2]. Among all novel technologies described for deep fuel desulphurization, adsorption appears as a soft technology for sulphur removal because hydrogen is not extensively required and mild operation conditions can be used. Several adsorption processes such as IRVAD or Phillips S-Zorb have been developed and industrially proven in order to complement or substitute HDS in refineries [2]. Adsorbents based on transition metals supported on silica gel and alumina have been explored for producing ultra-clean fuels and gasoline for fuel cell applications [3, 4].

π complexation adsorbents based on Y zeolite exchanged with Cu (I) and Ag have been used as selective adsorbents in diesel desulphurization [1, 5–7]. However, diffusivities of sulphur compounds present in heavy fuels into zeolite micropores are very small. In order to improve the adsorptive diffusion into the adsorbent, mesoporous Ag^{+}-SBA-15 has been tested in the adsorption of model refractory sulphur compounds such as dibenzothiophene (DBT) and 4,6-dimethyldibenzothiophene (4,6-DMDBT) [8]. Mesoporous aluminophosphates also appeared as good adsorbents in fuel desulphurization [9].

The aim of this work is to study the desulphurization of a LCO gas oil (515 ppmw of S) using mesoporous silica SBA-15 and mesoporous aluminophosphates impregnated with several transition metals (Ag, Cu and Ni) with different metal loadings. Equilibrium and fixed bed adsorption experiments were carried out and the main adsorption parameters have been calculated.

Experimental

Adsorbent preparation

Several mesoporous adsorbents have been synthesised using block copolymers as surfactants. Mesoporous SBA-15 has been prepared according to Stucky and co-workers [10]. Mesoporous aluminophosphates were synthesised using pluronic P-123 (Aldrich) following the procedure described by Tian et al. [11]. To synthesise mesoporous materials with higher pore diameters, Pluronic F-127 (Aldrich) has been used as a surfactant [12].

Mesoporous materials were impregnated with 5, 10 and 20 wt% of transition metal, using $AgNO_3$, $Ni(NO_3)_2 \cdot 6H_2O$, $Cu(NO_3)_2 \cdot 3H_2O$ as metal precursors dissolved in 25 g of ethanol per gram of the calcined material. The solvent was evaporated under vacuum and the recovered solids were calcined at 823 K.

Characterisation of the adsorbents

BET surface area was calculated from nitrogen adsorption–desorption measurements at 77 K using a Micromeritics Asap-2020 instrument. The pore size was calculated from desorption branches based on BJH method. X-ray diffraction (XRD) patterns were performed on a Philips diffractometer (X′pert MPD) with CuK_{α} radiation. TEM micrographs were acquired on a JEOL JEM-2000 FX microscope. Chemical composition was determined by X-ray fluorescence (XRF) in a PANalytical AXIOS wavelength-dispersive X-ray spectrometer.

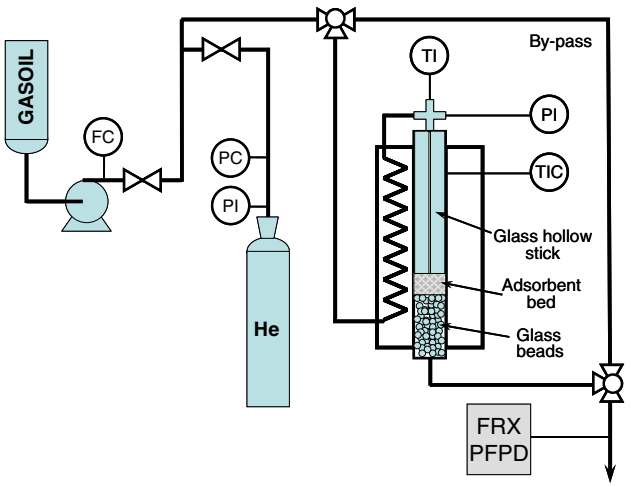

Fig. 1 Experimental set-up for dynamic experiments

Adsorption experiments

Equilibrium adsorption experiments were carried out in closed Pyrex tubes with Vyton seals, placed in a thermostatic bath. LCO gas oil was obtained from Repsol-YPF with a sulphur content of 515 ppmw. 2.5 g of this fuel was stirred with different weights of the adsorbents at 298 K during 7 days. Liquid phase sulphur analyses were performed by XRF, in a PANalytical AXIOS wavelength-dispersive X-ray spectrometer based on multi-layer analyser, using S-K_{α} spectral line in 27 mm PE-HD cells, with 2.5 μm Mylar film windows in helium mode. Sulphur compounds were analysed using a Varian CP-3800 gas chromatograph equipped with a capillary column, CP-Sil 5 CB (Chrompack, 45 m long and 0.53 mm i.d.) and a sulphur-specific pulsed flame photometric detector (PFPD).

Dynamic adsorption runs were carried out in a stainless steel down-flow fixed bed adsorber (Fig. 1), with an internal diameter of 9 mm and 25 cm length, placed in an oven and packed with 2 g of adsorbent. The temperature of the bed was controlled at 298 K. A positive displacement pump was used to feed the LCO into the bed at a constant flow rate of 0.5 cm^3 min^{-1}. The effluent was analysed by XRF and GC-PFPD.

Results and discussion

Adsorbents properties

Mesoporous SBA-15 and aluminophosphates were analysed by means of XRD in order to analyse their mesostructure. Figure 2 shows the XRD patterns of the solid powders obtained. SBA-15 material synthesised shows narrow and intense diffraction peaks (100, 110 and 200),

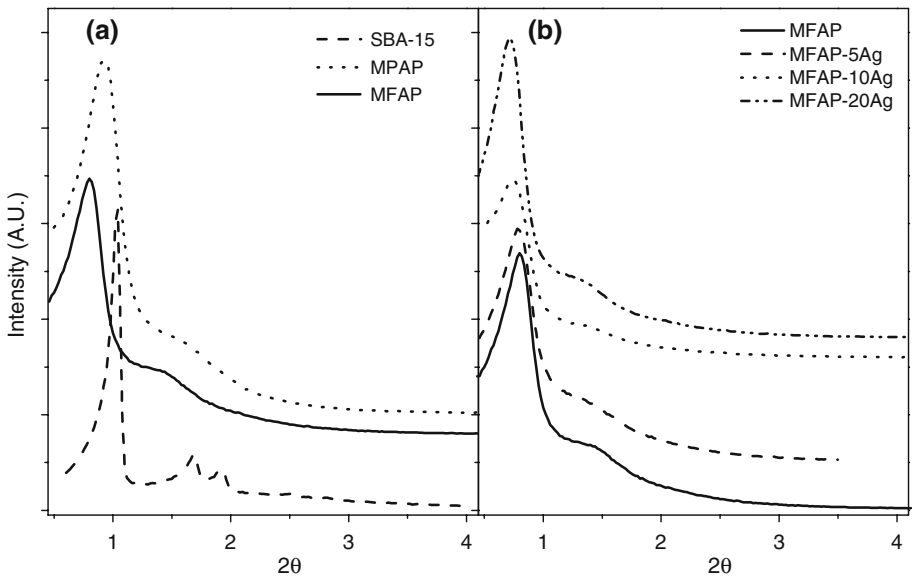

Fig. 2 XRD: **a** support materials and **b** MFAP materials impregnated with Ag

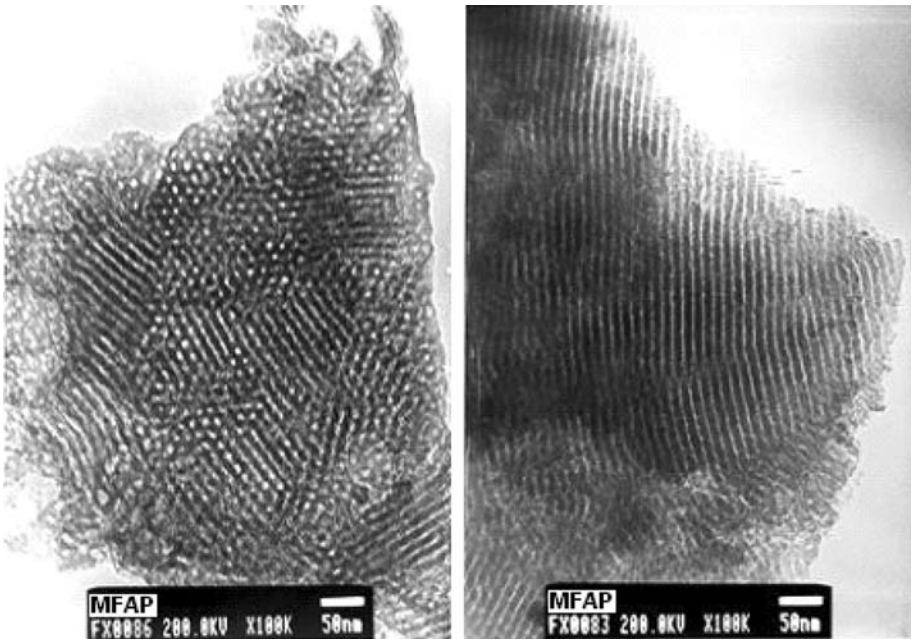

Fig. 3 TEM micrographs of MFAP sample

characteristic of a periodic hexagonal mesoporous material. Mesoporous aluminophosphates materials synthesised with amphiphilic block copolymers show an intense diffraction peak, characteristic of a periodic mesoporous material (100), being broad and indistinguishable the diffraction peaks 110 and 200. Nevertheless, Fig. 3 shows the TEM images of the MFAP sample, where the periodic hexagonal channels can be clearly distinguished.

The diffraction peak is displaced to lower angles when the template has higher molecular weight (lower angles for F-127 than P-123) indicating larger pores. SBA-15 presents a narrower peak due to its better hexagonal arrangement. Moreover, when the MFAP material was impregnated, the characteristic peak of the structure appeared at the same angles, which confirms that the impregnation procedure did not provoke the collapse of the structure.

Figure 4 presents the N_2 adsorption isotherms at 77 K of the synthesised materials. The N_2 adsorption isotherms of the materials present a type IV isotherm with a hysteresis loop. The p/p_0 position of the loop is clearly related to a diameter of the pores in the mesopore range, and the sharpness of the step indicates the uniformity of the pore size distribution. SBA-15 presents the narrower pore size distribution, which is also consistent with XRD measurements.

Chemical composition, surface specific area, pore volume and pore diameters of the selected adsorbents studied are summarised in Table 1.

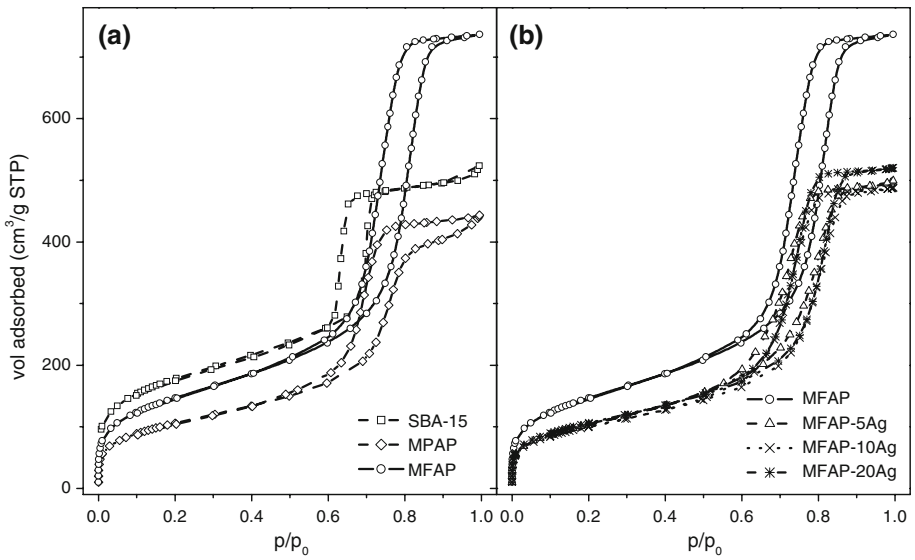

Fig. 4 N_2 adsorption–desorption isotherms at 77 K: **a** support materials and **b** MFAP materials impregnated with Ag

Table 1 Physical properties of the selected adsorbents

Adsorbent	P/Al (molar)	Ag (wt%)	BET area ($m^2\ g^{-1}$)	Pore volume ($cm^3\ g^{-1}$)	Pore diameter (nm)
SBA-15	–	0	668	1.06	6.4
MPAP	0.95	0	387	0.68	5.9
MFAP	0.97	0	536	1.14	7.1
MFAP-5Ag	0.97	5	379	0.77	6.6
MFAP-10Ag	0.97	10	364	0.75	7.0
MFAP-20Ag	0.97	20	387	0.80	7.0

Aluminophosphates synthesised using P-123 (MPAP) and F-127 (MFAP) show a P/Al molar ratio near to one. In those materials, P and Al are tetrahedrally coordinated corresponding to an ordered arrangement of the aluminophosphate framework. In all cases, materials synthesised using F-127 have larger pore sizes and pore volumes than those using P-123, due to the higher molecular weight of F-127.

In order to compare the influence of the adsorbent surface properties, SBA-15 silica and MPAP aluminophosphate with similar pore diameters have been synthesised.

The three basic materials have been impregnated with different loadings of Ag, Ni and Cu; only the characterisation results of the best adsorbents have been included in this article. The impregnating procedure provokes a reduction in the BET surface areas of a 20%. In order to explain the reduction in surface areas, TEM micrographs of Ag-impregnated mesoporous aluminophosphates with different silver contents have been obtained (Fig. 5). The dark dots present in the images are the silver particles generated after calcination. As it can be seen in the figures the amount and the size of the particles increase as the silver content is doubled. The Ag particle size is less than the pore diameter calculated from the N_2 adsorption–desorption isotherm (*ca.* 6.5 nm), hence the overall impregnation process from the impregnation to the final calcinations provokes this reduction.

Adsorption experiments

In order to select the best adsorbent for desulphurization purposes, comparative equilibrium adsorption experiments were carried out. The selected adsorbent was deeper studied in dynamic and equilibrium experiments.

Adsorbent selection

Figure 6 presents the equilibrium capacity of adsorption (q_D) and the desulphurization degree (DES) of the 5% Ag-impregnated adsorbents.

Mesoporous aluminophosphates show higher adsorption capacities and degrees of desulphurization than those obtained for SBA-15; moreover, the Ag-impregnated materials follow the same variation, although the differences between the Ag-impregnated materials are smaller than the as-synthesised ones due to the high desulphurization levels

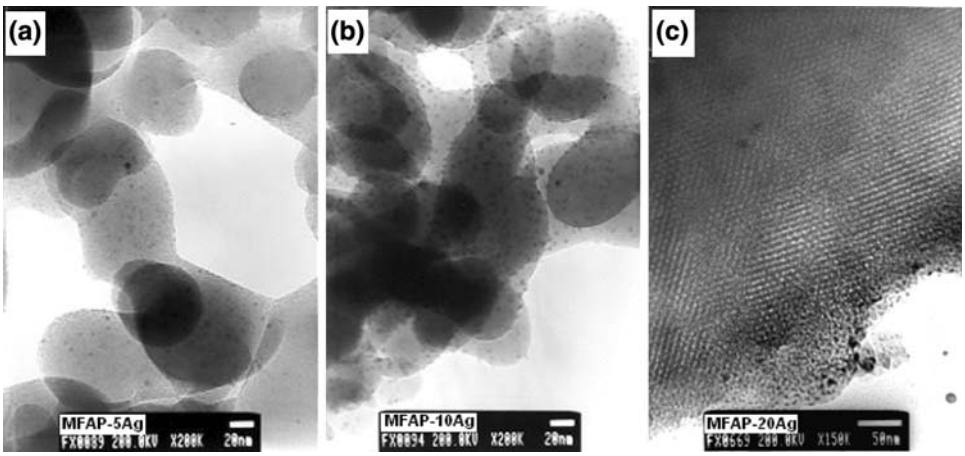

Fig. 5 TEM images of aluminophosphates impregnated with different silver contents: **a** MFAP-5Ag, **b** MFAP-10Ag and **c** MFAP-20Ag

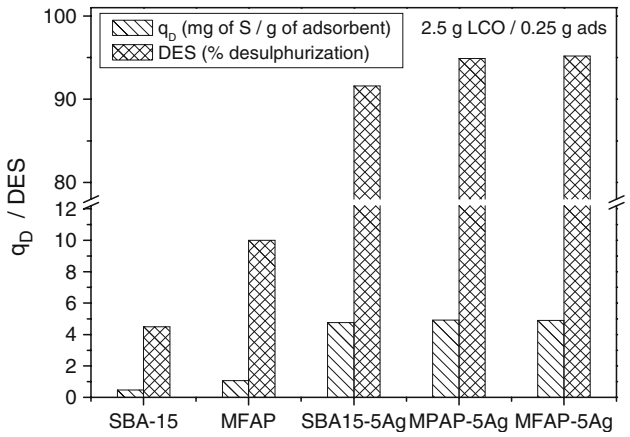

Fig. 6 Support influence on the desulphurization performance

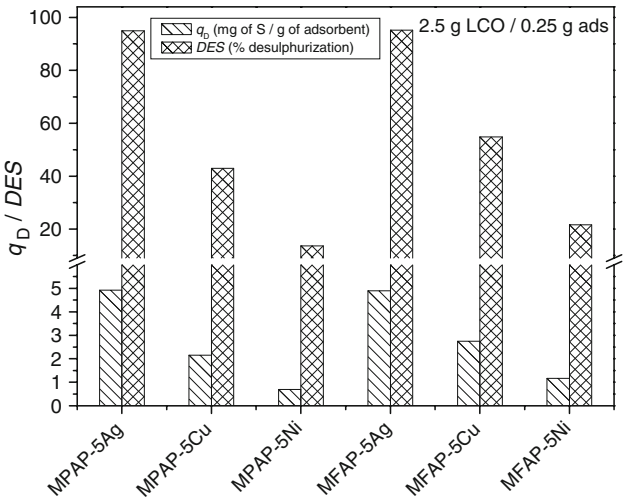

Fig. 7 Impregnated metal influence on the desulphurization performance

obtained for this Ag content. This trend can be explained considering that sulphur compounds are polar and therefore would be better adsorbed onto more polar adsorbents such as aluminophosphates [9, 13].

Among the aluminophosphates, the adsorbent with the highest pore diameter (MFAP) presents the highest sulphur adsorption capacity. These results suggest that sulphur compounds present in heavy fuels cannot diffuse easily into the pores.

Figure 7 shows the influence of the transition metal impregnated onto mesoporous aluminophosphates on the desulphurization performance. As can be seen, Ag-impregnated adsorbents showed the best desulphurization results, followed by copper and nickel impregnated materials.

These results present opposite trend than those obtained before by Yang and co-workers in desulphurization of fuels with transition metal ion exchanged zeolites, where Y zeolite exchanged with Cu^+ showed higher adsorption capacities than the Y zeolite exchanged with Ag^+ [5–7]. This result was explained considering the enthalpy of adsorption of a model organosulphur compound onto these adsorbents. The fact that our adsorbents have not been calcined in reductive conditions and therefore Cu^+ was not produced could explain the different trend observed.

Figure 8 presents the influence of the Ag loading onto MFAP materials. As can be seen, the impregnation enhances the adsorption capacity notably and therefore the desulphurization level. However, a high Ag content only provokes a slight increment in desulphurization degrees. Hence, an adsorbent impregnated with a 5% of Ag presents higher adsorption capacities per gram of silver than those obtained for a 20% Ag-impregnated adsorbent.

Adsorption isotherms and dynamic experiments

Adsorption isotherms of LCO on MFAP-5Ag, MPAP-5Ag and MFAP-10Ag samples are shown in Fig. 9. According to the Giles classification of solution adsorption isotherms [14], the adsorbents present a type L isotherm, which is characteristic of systems with highly polar solutes and substrates in a non-polar solvent.

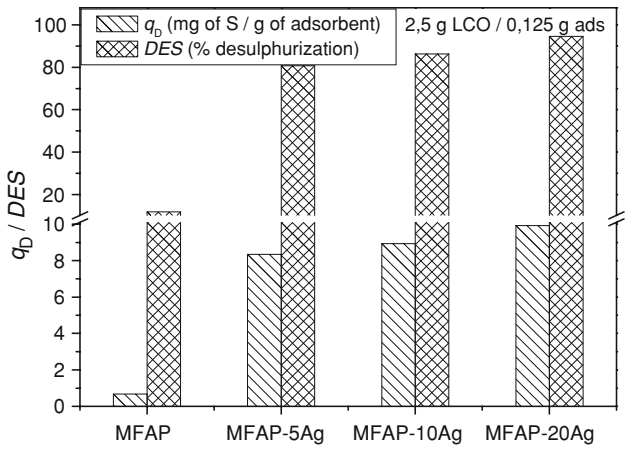

Fig. 8 Metal loading influence on the desulphurization performance

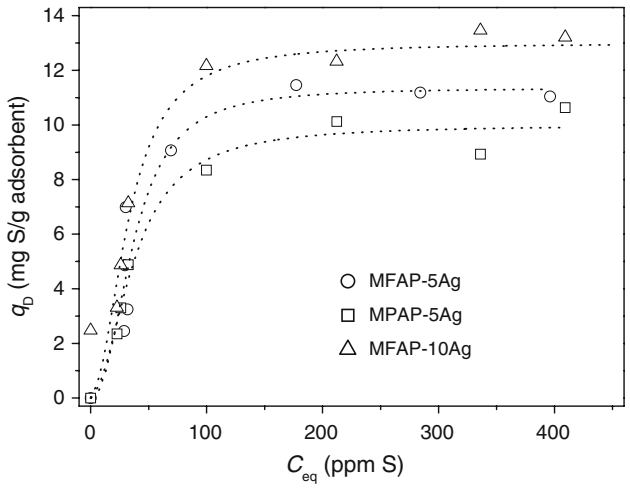

Fig. 9 Adsorption isotherms of sulphur present in LCO onto Ag-impregnated aluminophosphates

The equilibrium experimental data have been fitted to the Langmuir-Freundlich adsorption isotherm (dot lines in Fig. 9):

$$q_D = \frac{q_{max} \cdot (K \cdot C_{eq})^n}{1 + (K \cdot C_{eq})^n} \quad (1)$$

where, q_D is the adsorption capacity at a given equilibrium concentration (C_{eq}), q_{max} is the maximum adsorption capacity and K is the adsorption equilibrium constant. n describes the adsorption binding interactions among adsorbing compounds. For independent non-interacting adsorption sites corresponding to the Langmuir model, the value n is 1. When $n > 1$, positive cooperative adsorption is assumed, while when $0 < n < 1$ negative cooperative adsorption can be expected. These parameters were obtained and listed in Table 2.

The maximum adsorption capacity (q_{max}) of MFAP-5Ag is higher than MPAP-5Ag one due to the higher surface area and pore size of that adsorbent (Table 1). When the amount of Ag impregnated onto the MFAP matrix is doubled, the maximum adsorption capacity increases too; however, this variation is much lower than the Ag increment. Although the Ag content is higher and should favour the sulphur adsorption, a higher Ag content could lead to bigger particles with a less external surface and therefore less adsorption sites per gram of metal. In all cases, the parameter n is higher than 1 indicating that there is a cooperative adsorption between the organosulphur compounds adsorbed and the adsorbent surface.

Table 2 Parameters obtained from Langmuir-Freundlich equation

Adsorbent	q_{max} (mg g^{-1})	K (ppm^{-n})	n	r^2
MFAP-5Ag	11.36 ± 1.00	0.027 ± 0.005	2.28 ± 1.15	0.917
MPAP-5Ag	10.00 ± 0.53	0.027 ± 0.004	1.94 ± 0.56	0.980
MFAP-10Ag	13.00 ± 1.05	0.031 ± 0.005	2.03 ± 1.07	0.903

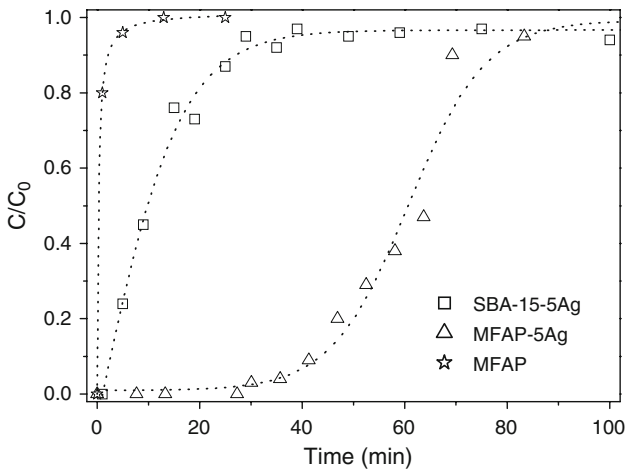

Fig. 10 Breakthrough curves of sulphur compounds present in LCO onto different adsorbents

Breakthrough curves of sulphur compounds present in LCO onto different adsorbents are shown in Fig. 10. Adsorption capacities at saturation time, q_{sat}, and at breakthrough time, q_{br}, as well as the fractional bed utilisation, FBU, defined as the ratio q_{br}/q_{sat} have been obtained. These parameters and the adsorption capacity deduced from the isotherm ($q_{D.eq}$) are listed in Table 3.

The adsorption capacity of the as-synthesised materials in dynamic experiments is almost negligible compared with the Ag-impregnated ones, as it was previously observed in equilibrium experiments (Fig. 8).

The saturation and the breakthrough time capacities depend on the adsorbent polarity for adsorbents with the same Ag content. Mesoporous aluminophosphates present more polar surfaces and therefore lead to higher capacities than mesoporous silica SBA-15.

Table 3 Adsorption parameters obtained from the breakthrough curve

Adsorbent	C_0 (ppm S)	$q_{D.eq}$ (mg g^{-1})	q_{br} (mg g^{-1})	q_{sat} (mg g^{-1})	FBU
MFAP	515	–	0	0.14	0.0
MFAP-5Ag	515	11.36	4.25	7.06	0.60
SBA-15-5Ag	515	–	0.16	1.82	0.09

Conclusions

Selective adsorbents for HDS refractory sulphur compounds removal have been prepared from ordered mesoporous materials. The adsorbent composition has an important effect on desulphurization; mesoporous adsorbents based on Al and P present higher adsorption capacities than mesoporous SBA-15. Ag-impregnated materials showed better adsorption properties than those impregnated with Cu and Ni. The mesoporous aluminophosphate impregnated with a 5% of Ag (MFAP-5Ag) presents a favourable adsorption isotherm of LCO sulphur compounds with a maximum adsorption capacity of 11.36 mg of sulphur per gram of adsorbent.

In fixed bed adsorption experiments, the presence of Ag supported on the mesoporous materials enhanced the saturation adsorption capacity achieved. MFAP-5Ag showed a breakthrough and a saturation capacity of 4.25 and 7.06 mgS/g, respectively. The high breakthrough capacity of MFAP-5Ag for diesel fuel (which contains refractory sulphur compounds to HDS) reinforces adsorption as a complementary technology to HDS for diesel desulphurization.

Acknowledgements Financial support from E.U. and Comunidad Autónoma de Madrid through the projects FEDER European Project 2FD1997-1873 and CAM 07 M/0056/2001 is gratefully acknowledged.

References

1. Hernández-Maldonado AJ, Yang RT (2004) AIChE J 50:791
2. Babich IV, Moulijn JA (2003) Fuel 82:607
3. Ma X, Sun L, Song C (2002) Catal Today 77:107
4. Zhang JC, Song LF, Hu JY, Ong SL, Ng WJ, Lee LY, Wang YH, Zhao JG, Ma RY (2005) Energy Convers Manag 46:1
5. Yang RT, Hernández-Maldonado AJ, Yang FH (2003) Science 301:79
6. Hernández-Maldonado AJ, Yang RT (2003) Ind Eng Chem Res 42:123
7. Yang RT, Takahashi A, Yang FH (2001) Ind Eng Chem Res 40:6236
8. McKinley SG, Angelici RJ (2003) Chem Commun 2620
9. Sotelo JL, Uguina MA, Águeda VI, Serrano J (2005) Stud Surf Sci Catal 158B:1089
10. Zhao E, Feng J, Huo Q, Melosh N, Fredrickson GH, Chemelka BF, Stucky GD (1998) Science 279:548
11. Tian B, Liu X, Tu B, Yu C, Fan J, Wang L, Xie S, Stucky GD, Zhao D (2003) Nat Mater 2:159
12. Wang L, Tian B, Fan J, Liu X, Yang H, Yu C, Tu B, Zhao D (2004) Microporous Mesoporous Mater 67:123
13. Sotelo JL, Uguina MA, Águeda VI (2002) XXVII Reunión Ibérica de adsorción 151
14. Giles CH, MacEwan TH, Nakhwa SN, Smith D (1960) J Chem Soc 3973